



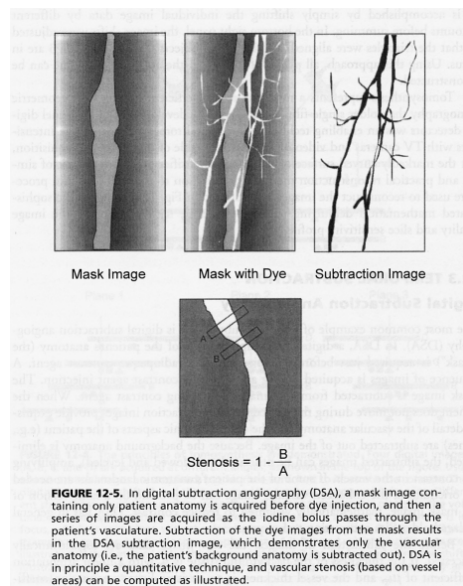
ENGG 167 - F02
MEDICAL IMAGING

Wednesday, Oct. 27

Chapter 14: Computed Tomography

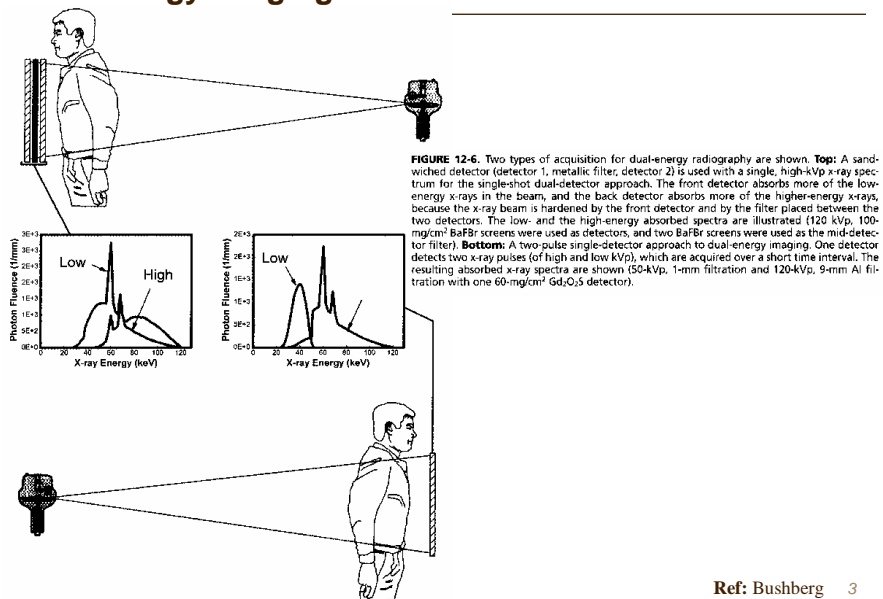
Reference: Chapters 12 & 13, *The Essential Physics of Medical Imaging*, Bushberg
Computed Tomography, Kalender, Verlag, 2000.
 Chapter 12, *Intermediate Physics for Medicine and Biology*, 3rd Ed., Hobbie.
 Chapter 3, *Principles of Computerized Tomographic Imaging*, Kak and Slaney, IEEE Press ¹

X-ray imaging with digital subtraction



Ref: Bushberg 2

Dual energy imaging



Dual energy subtraction imaging

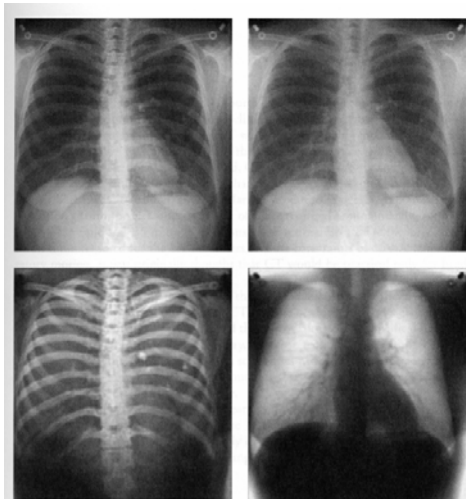


FIGURE 12-7. Dual-energy images are shown. The upper left image is the low-energy image (56 kVp); the upper-right image is the high-energy image (120 kVp, 1 mm Cu). The lower left image shows the energy subtraction image weighted to present bone only, and on the lower right is the tissue-weighted image. This patient had a calcified granuloma that is well seen on the bone-only image. The soft tissue image shows the lung parenchyma without the overlaying ribs as a source of distraction.

Ref: Bushberg 4

Chapter 12 – Tomosynthesis – approaching computed tomography

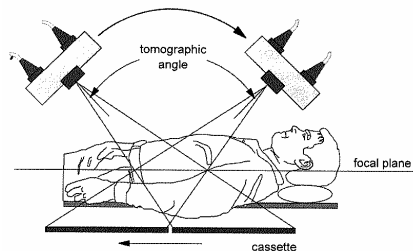


FIGURE 12-1. The motion of the x-ray tube and cassette that occurs in geometric tomography is illustrated. The focal plane is the location of the tomographic slice, and this occurs at the pivot point of the machine.

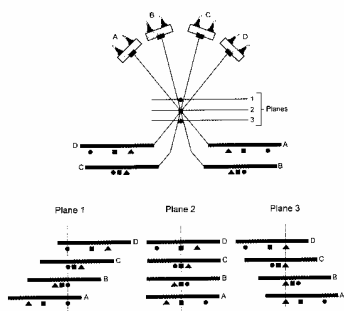


FIGURE 12-4. The principles of tomosynthesis are demonstrated. Four digital images (A, B, C, and D) are acquired at different angles, as shown in the top of the figure. Usually about ten images are acquired, but four are sufficient to illustrate the concept. The digital images are shifted and then summed to produce tomographic images. Different shift distances can be used to reconstruct different tomographic planes in the volume. For example, with no shift distance, the images are aligned and plane 2 is in focus, which is coincident with the focal plane of the scan; plane 2 is just a digital example of regular geometric tomography. Plane 1 is focused using the shift distances illustrated at the bottom left of the figure, and plane 3 can be focused using the shifts illustrated at the bottom right. After shifting the images in the computer, they are added to produce the tomographic image.

Ref: Bushberg

5

Computed Tomography – READ Chapter 13

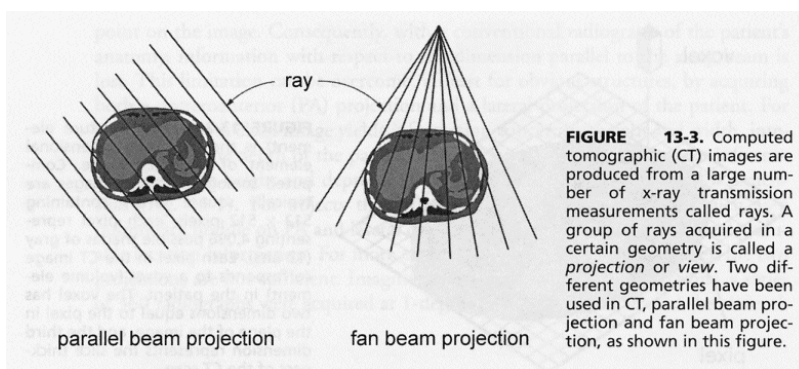
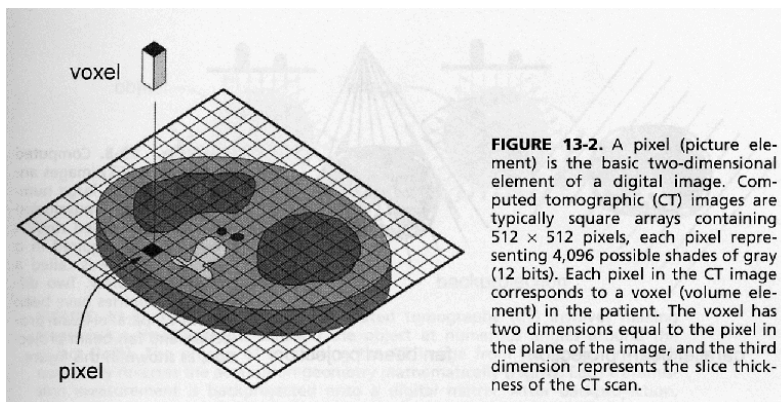


FIGURE 13-3. Computed tomographic (CT) images are produced from a large number of x-ray transmission measurements called rays. A group of rays acquired in a certain geometry is called a *projection* or *view*. Two different geometries have been used in CT, parallel beam projection and fan beam projection, as shown in this figure.

Ref: Bushberg 6

Computed Tomography: reconstruct pixelated images



Ref: Bushberg 7

Computed Tomography – detection geometries

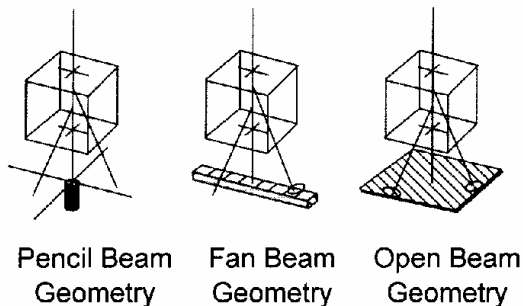
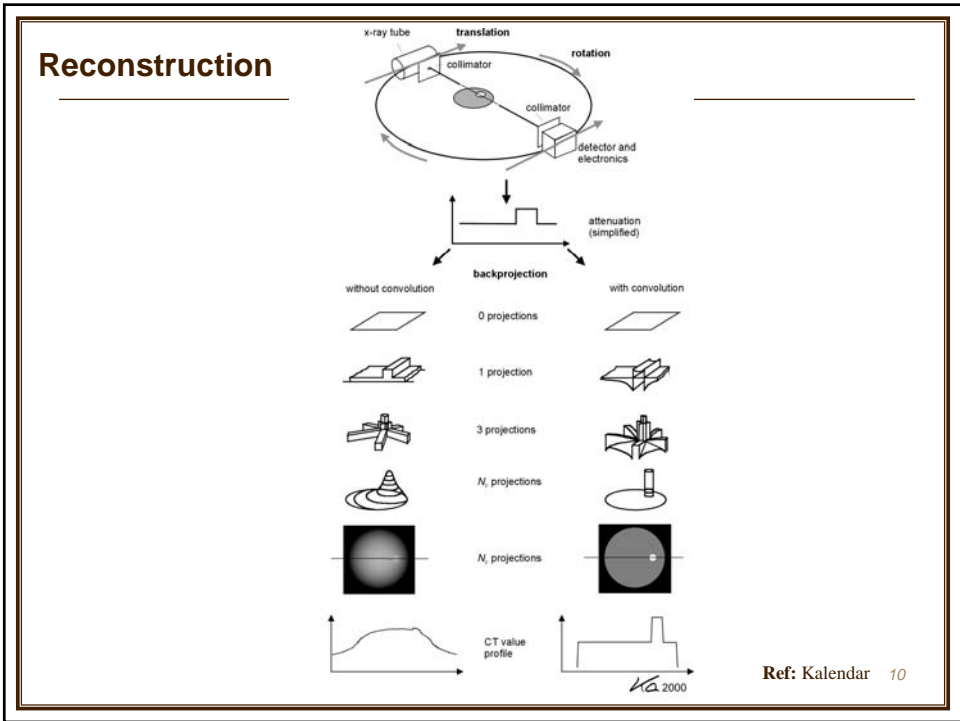
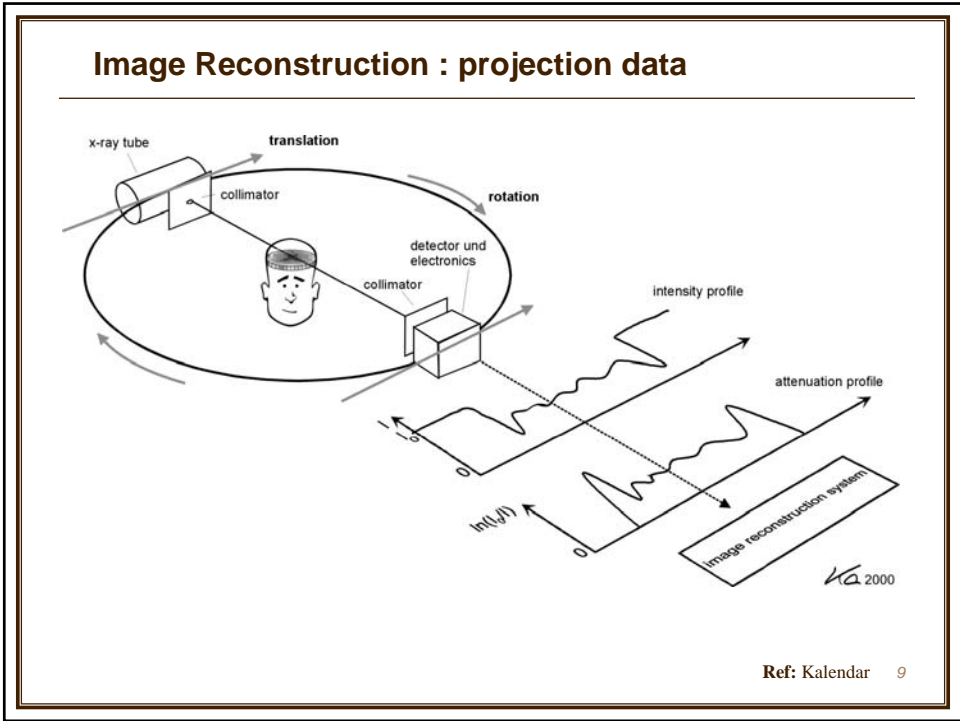
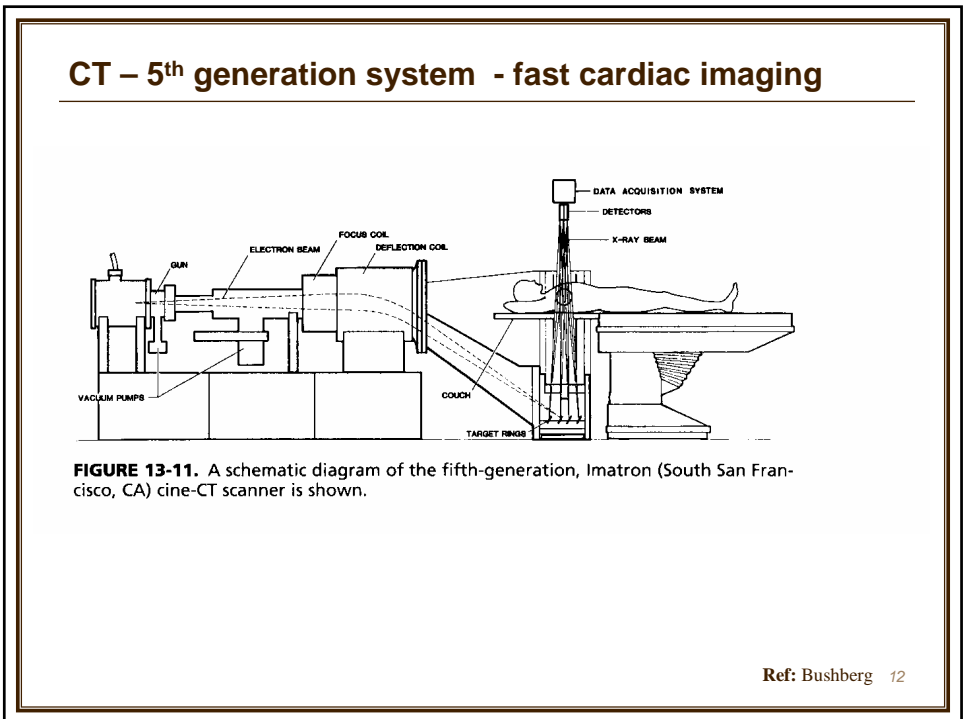
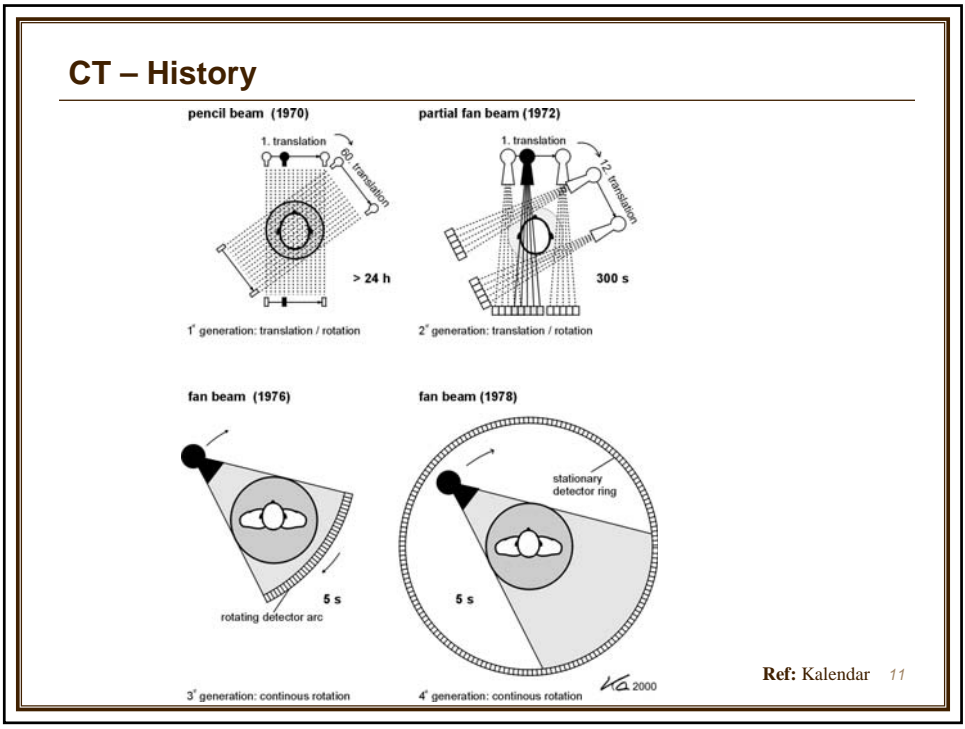


FIGURE 13-6. Pencil beam geometry makes inefficient use of the x-ray source, but it provides excellent x-ray scatter rejection. X-rays that are scattered away from the primary pencil beam do not strike the detector and are not measured. Fan beam geometry makes use of a linear x-ray detector and a divergent fan beam of x-rays. X-rays that are scattered in the same plane as the detector can be detected, but x-rays that are scattered out of plane miss the linear detector array and are not detected. Scattered radiation accounts for approximately 5% of the signal in typical fan beam scanners. Open beam geometry, which is used in projection radiography, results in the highest detection of scatter. Depending on the dimensions and the x-ray energy used, open beam geometries can lead to four detected scatter events for every detected primary photon ($s/p=4$).

Ref: Bushberg 8





CT – 6th generation - helical or spiral CT

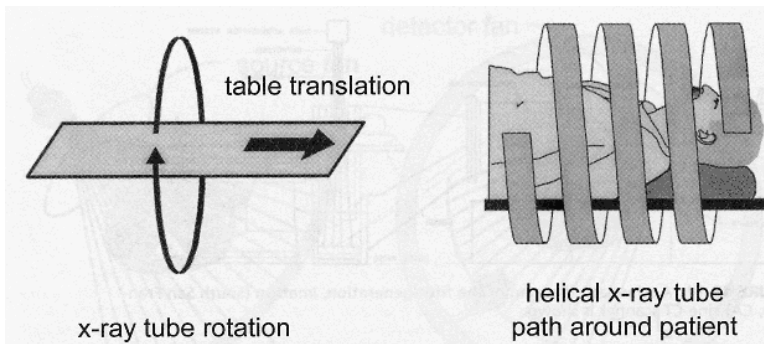


FIGURE 13-12. With helical computed tomographic scanners, the x-ray tube rotates around the patient while the patient and the table are translated through the gantry. The net effect of these two motions results in the x-ray tube traveling in a helical path around the patient.

Ref: Bushberg 13

CT – 7th generation – multiple detector slice arrays

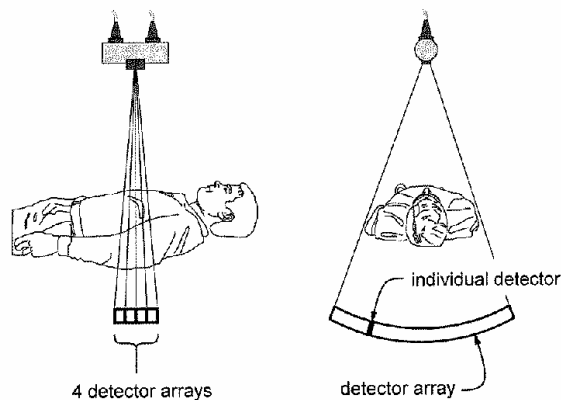
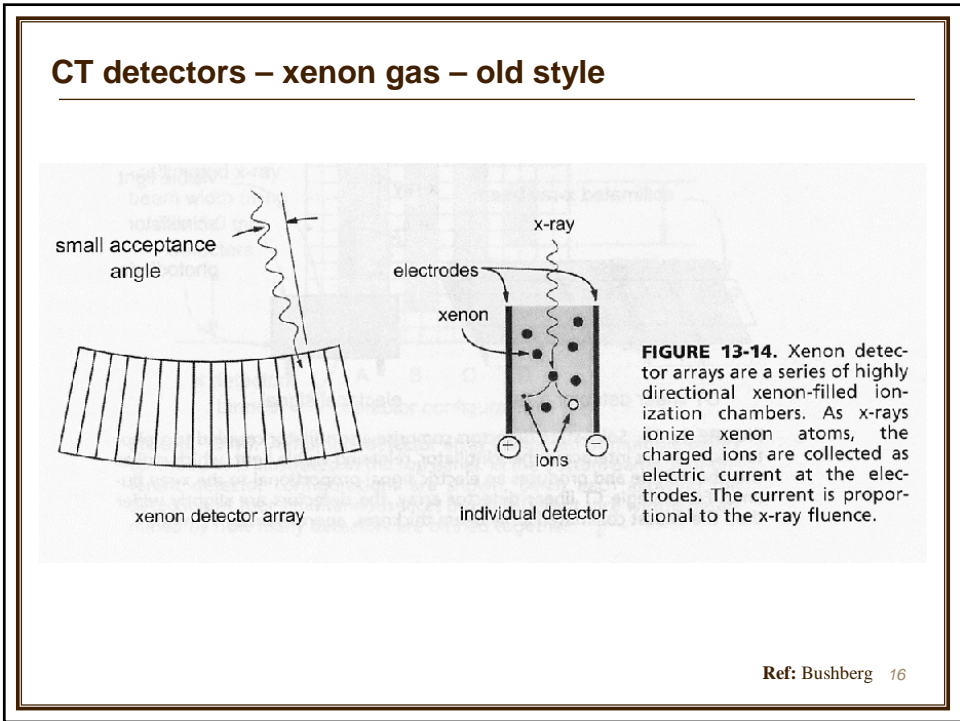
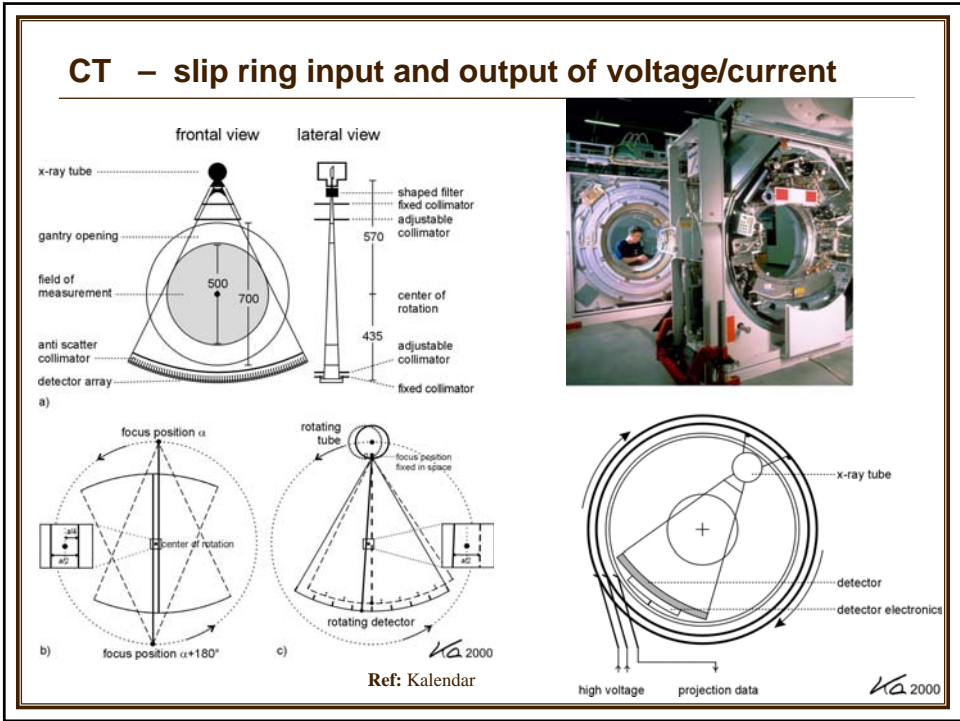


FIGURE 13-13. Multiple detector array computed tomographic (CT) scanners use several, closely spaced, complete detector arrays. With no table translation (nonhelical acquisition), each detector array acquires a separate axial CT image. With helical acquisition on a multiple detector array system, table speed and detector pitch can be increased, increasing the coverage for a given period of time.

Ref: Bushberg 14



CT detectors – solid state detectors

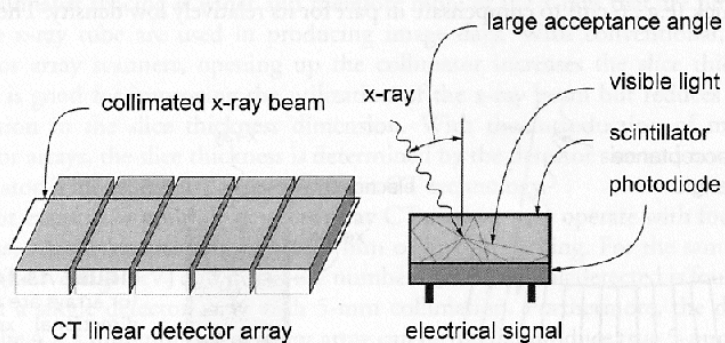


FIGURE 13-15. Solid-state detectors comprise a scintillator coupled to a photodiode. X-rays interact in the scintillator, releasing visible light, which strikes the photodiode and produces an electric signal proportional to the x-ray fluence. For a single CT linear detector array, the detectors are slightly wider than the widest collimated x-ray beam thickness, approximately 12 mm.

Ref: Bushberg 17

CT detectors – solid state multiple detector arrays

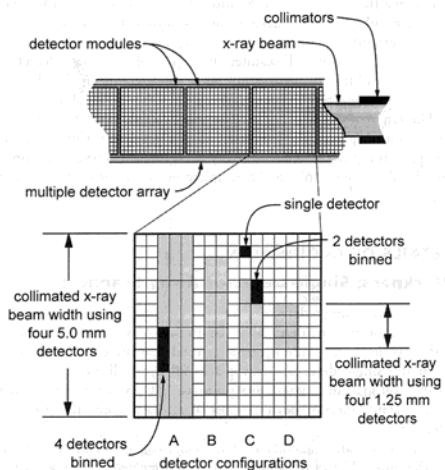


FIGURE 13-16. A multiple detector array composed of multiple detector modules is illustrated in the top panel. In the bottom panel, four different detector configurations are shown, (A–D) each allowing the detection of four simultaneous slices but at different slice widths determined by how many detectors are binned together.

Ref: Bushberg 18

CT slice thickness

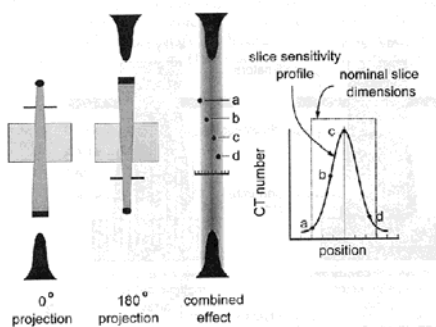


FIGURE 13-17. The slice sensitivity profile is a result of detector width; focal spot size and distribution; collimator penumbra, and the combined influence of all the projection angles. The nominal slice dimensions convey that the computed tomographic (CT) image is of a slab of tissue of finite thickness; however, the same object at different locations in the slice volume (e.g., positions A, B, C, and D) will produce different CT numbers in the image. Consequently, when a small object is placed in the center of the CT slice, it produces greater contrast from background (greater difference in CT number) than when the same object is positioned near the edge of the slice volume.

Increasing slice thickness increases SNR by square root of thickness ratio. This provides better contrast resolution but decreased spatial resolution in slice thickness dimension. Alternatively, the mAs can be increased for thin slices to keep the number of counts detected high.

Slice thickness is actually a sensitivity distribution

Ref: Bushberg 19

CT slice thickness & collimators

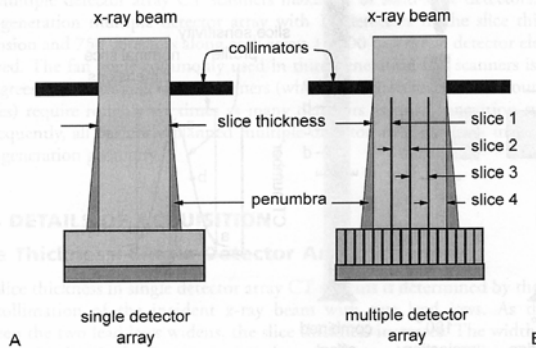


FIGURE 13-18. A: In a single detector array computed tomography (CT) scanner, the width of the CT slice is determined by the collimator. With single detector array scanners, the collimator width is always smaller than the maximum detector width. **B:** Multiple detector array CT scanners acquire several slices simultaneously (four slices shown here), and the x-ray beam collimation determines the outer two edges of the acquired slices. Slice thickness is changed in the single detector array by mechanically changing the collimator position. Slice thickness is determined in the multiple detector array scanner by binning different numbers of detector subunits together and by physically moving the collimator to the outer edges of all four slices.

Ref: Bushberg 20

Pitch -Major factor influencing patient dose, image quality and scan time

$$\text{Collimator pitch} = \frac{\text{table movement (mm) per 360-degree rotation of gantry}}{\text{collimator width (mm) at isocenter}}$$

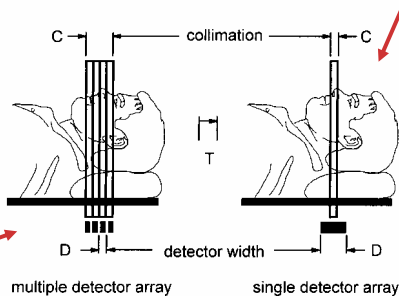


FIGURE 13-19. With a single detector array computed tomographic (CT) scanner, the collimation width is always narrower than the maximum single detector width. A multiple detector array scanner uses collimation that is always wider than a single detector array width. Letting T represent the table translation distance during a 360-degree rotation of the gantry, C would be the collimation width and D would be the detector width. Collimator pitch is defined as T/C, and detector pitch is defined by T/D. For a multiple detector array CT scanner with four detector arrays, a collimator pitch of 1.0 is equal to a detector pitch of 4.0.

$$\text{Detector pitch} = \frac{\text{table movement (mm) per 360-degree rotation of gantry}}{\text{detector width (mm)}}$$

$$\text{Collimator pitch} = \frac{\text{Detector pitch}}{N}$$

Ref: Bushberg 21

Interpolation of data in spiral CT

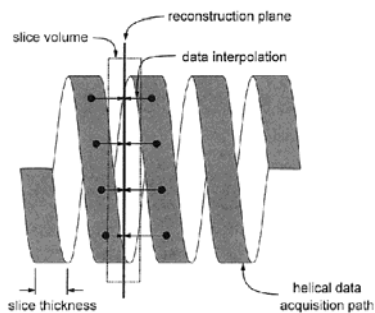


FIGURE 13-25. During helical acquisition, the data are acquired in a helical path around the patient. Before reconstruction, the helical data are interpolated to the reconstruction plane of interest. Interpolation is essentially a weighted average of the data from either side of the reconstruction plane, with slightly different weighting factors used for each projection angle.

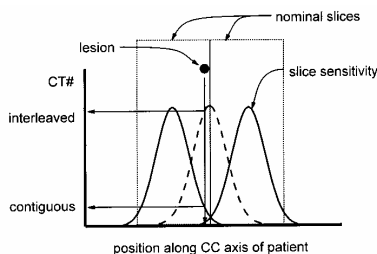


FIGURE 13-26. This figure illustrates the value of interleaved reconstruction. The nominal slice for contiguous computed tomographic (CT) images is illustrated conceptually as two adjacent rectangles; however, the sensitivity of each CT image is actually given by the slice sensitivity profile (solid lines). A lesion that is positioned approximately between the two CT images (black circle) produces low contrast (i.e., a small difference in CT number between the lesion and the background) because it corresponds to low slice sensitivity. With the use of interleaved reconstruction (dashed line), the lesion intersects the slice sensitivity profile at a higher position, producing higher contrast.

Ref: Bushberg 22

Reconstruction - increasing # rays increases resolution

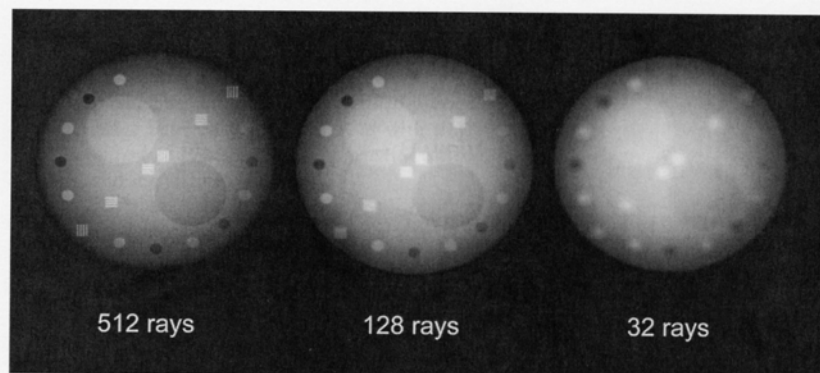


FIGURE 13-22. An image of a test object is shown, reconstructed with 960 views in each image, but with the number of rays differing as indicated. As the number of rays is reduced, the detector aperture was made wider to compensate. With only 32 rays, the detector aperture becomes quite large and the image is substantially blurred as a result.

Ref: Bushberg 23

Reconstruction - increasing # views increases resolution

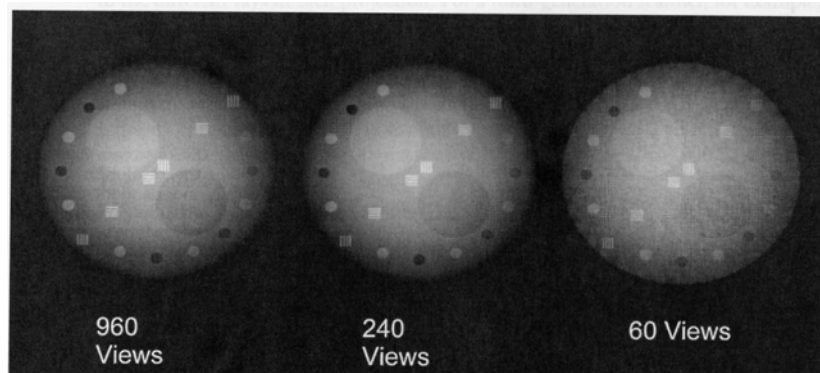


FIGURE 13-23. Each of the three images was reconstructed using 512 rays but differing numbers of views. In going from 960 to 240 views, a slight degree of view aliasing is seen (**center image**). When only 60 views are used (**right image**), the view aliasing is significant. The presence of the aliasing is exacerbated by objects with sharp edges, such as the line pair phantom in the image.

Ref: Bushberg 24

Reconstruction - effect of frequency filters

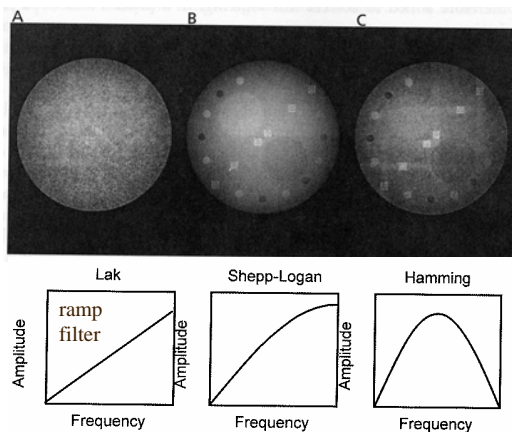


FIGURE 13-29. Three computed tomography (CT) reconstruction filters are illustrated. The plot of the reconstruction filter is shown below, with the image it produced above. **(A)** The Lak is the ideal reconstruction filter in the absence of noise. However, with the quantum noise characteristic in x-ray imaging including CT, the high-frequency components of the noise are amplified and the reconstructed image is consequently very noisy. **(B)** The Shepp-Logan filter is similar to the Lak filter, but roll-off occurs at the higher frequencies. This filter produces an image that is a good compromise between noise and resolution. **(C)** The Hamming filter has extreme high frequency roll-off.

Ref: Bushberg 25

Hounsfield units / CT Numbers

CT Numbers or Hounsfield Units

After CT reconstruction, each pixel in the image is represented by a high-precision floating point number that is useful for computation but less useful for display. Most computer display hardware makes use of integer images. Consequently, after CT reconstruction, but before storing and displaying, CT images are normalized and truncated to integer values. The number $CT(x,y)$ in each pixel, (x,y) , of the image is converted using the following expression:

$$CT(x,y) = 1,000 \frac{\mu(x,y) - \mu_{water}}{\mu_{water}}$$

where $\mu(x,y)$ is the floating point number of the (x,y) pixel before conversion, μ_{water} is the attenuation coefficient of water, and $CT(x,y)$ is the CT number (or Hounsfield unit) that ends up in the final clinical CT image. The value of μ_{water} is about 0.195 for the x-ray beam energies typically used in CT scanning.

<http://www.nobel.se/medicine/laureates/1979/hounsfield-lecture.pdf>

Ref: Bushberg 26

Hounsfield units / CT Numbers

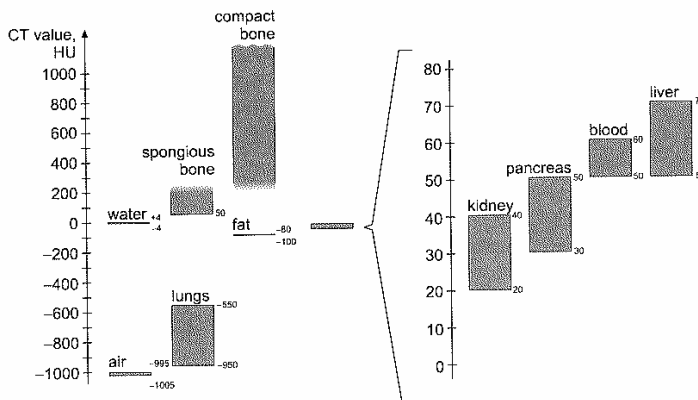
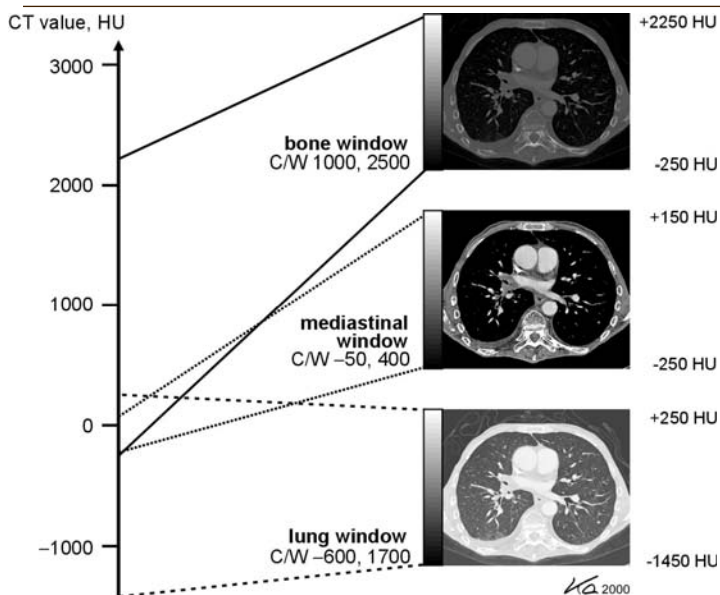


Figure 1.9
The Hounsfield scale. CT values characterize the linear attenuation coefficient of the tissue in each volume element relative to the μ -value of water. The CT values of different tissues are therefore defined to be relatively stable and to a high degree independent of the x-ray spectrum.

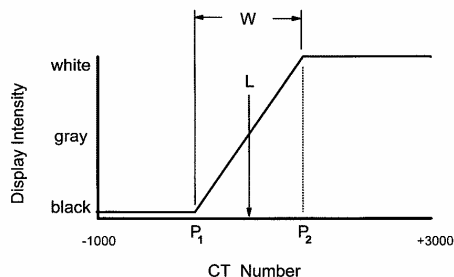
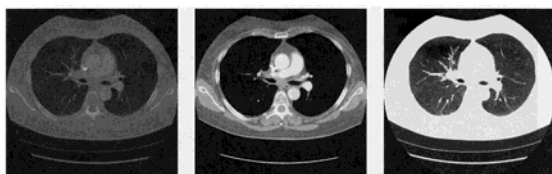
Ref: Kalender 27

Hounsfield units / CT Numbers



Ref: Kalender 28

CT Numbers – windowing for display



CT images – 12 bit
Human vision – 6-8 bit
Digital display – 8 bit

FIGURE 13-32. The concept of how the window and level values are used to manipulate the contrast of the CT image is illustrated. The *level* is the CT number corresponding to the center of the *window*. A narrow window produces a very high contrast image, corresponding to a large slope on the figure. CT numbers below the window (lower than P_1) will be displayed on the image as black; CT numbers above the window (higher than P_2) will be displayed as white. Only CT numbers between P_1 and P_2 will be displayed in a meaningful manner. The thoracic CT images (top) illustrate the dramatic effect of changing the window and level settings.

Ref: Bushberg 29

CT geometry

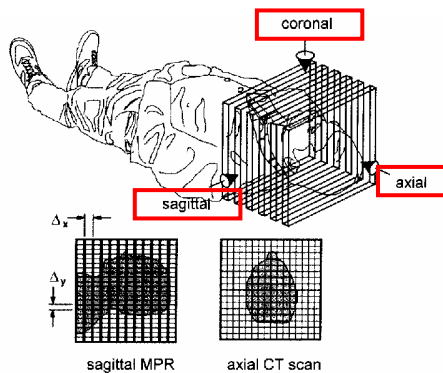


FIGURE 13-33. The coronal, sagittal, and axial projections are illustrated for reference. Both computed tomographic (CT) scans are produced as axial images, and within the image the pixel-to-pixel spacing is small (perhaps 0.5 mm, as a very general number). Coronal or sagittal multiplanar reconstructions (MPRs) can be produced from a series of axial CT scans. For instance, in a sagittal MPR image (bottom left), the vertical pixel spacing (Δy) is equivalent to the spacing of the pixels on the axial image. The horizontal spacing (Δx) corresponds to the distance between the reconstructed images. Because Δy is usually much smaller than Δx , it is common to interpolate image data in the horizontal dimension to produce square pixels. For MPR when helical acquisition was used, it is advantageous to reconstruct the images with a significant degree of interleave.

Ref: Bushberg 30

Radiation Dose in CT

Dose Measurement

Compton scattering is the principal interaction mechanism in CT, so the radiation dose attributable to scattered radiation is considerable, and it can be higher than the radiation dose from the primary beam. Scattered radiation is not confined to the collimated beam profile as primary x-rays are, and therefore the acquisition of a CT slice delivers a considerable dose from scatter to adjacent tissues, outside the primary beam. Furthermore, most CT protocols call for the acquisition of a series of near-contiguous CT slices over the tissue volume under examination. Take, for example, a protocol in which ten 10-mm CT slices are acquired in the abdomen. The tissue in slice 5 will receive both primary and scattered radiation from its acquisition, but it will also receive the scattered radiation dose from slices 4 and 6, and to a lesser extent from slices 3 and 7, and so on (Fig. 13-35).

The *multiple scan average dose* (MSAD) is the standard for determining radiation dose in CT. The MSAD is the dose to tissue that includes the dose attributable to scattered radiation emanating from all adjacent slices. The MSAD is defined as the average dose, at a particular depth from the surface, resulting from a large series

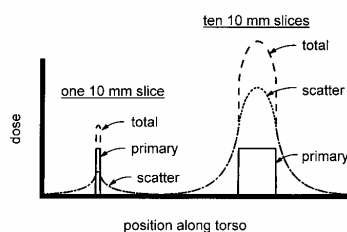


FIGURE 13-35. The radiation dose to the patient is shown as a function of position in the torso along the cranial-caudal dimension. The dose profile for one 10-mm slice is shown on the left, and the dose profile for ten contiguous 10-mm slices is shown on the right. The contribution (height) of the dose profile from the primary component is the same. However, with a number of adjacent slices, the scattered radiation tails build up and increase the total dose in each CT slice.

Ref: Bushberg 31

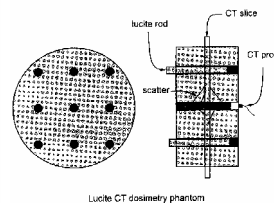
Radiation Dose in CT

An estimate of the MSAD can be accomplished with a single scan by measuring the *CT dose index* (CTDI). It can be shown that the CTDI provides a good approximation to the MSAD when the slices are contiguous. The CTDI measurement seeks to measure the scattered radiation dose from adjacent CT slices in a practical manner. The CTDI is defined by the U.S. Food and Drug Agency (21 CFR § 1 1020.33) as the radiation dose to any point in the patient including the scattered radiation contribution from 7 CT slices in both directions, for a total of 14 slices. In this text, this definition is referred to as the CTDI_{FDA}. One method to measure the CTDI_{FDA} is with many small thermoluminescent dosimeters (TLDs) placed in holes along 14-slice-thickness increments in a Lucite dose phantom. (TLDs are discussed in Chapters 20 and 23.) A single CT image is acquired at the center of the rod containing the TLDs, and the CTDI_{FDA} is determined from this single CT scan by summing the TLD dose measurements.

Medical physicists usually measure the CTDI with the use of a long (100 mm), thin *pencil ionization chamber*. The pencil chamber is long enough to span the width of 14 contiguous 7-mm CT scans and provides a good estimation of the CTDI_{FDA} for 7- and 8-mm slices. A single CT image is acquired at the center of the pencil chamber, and the CTDI is determined from this single CT scan. To calculate the CTDI, all of the energy deposition along the length of the ion chamber is assigned to the thickness of the CT slice:

$$CTDI = fX/T \times L$$

where X is the measured air kerma (mGy) or exposure (R) to the pencil ion chamber, f is an air-kerma-to-dose (mGy/mGy) or exposure-to-dose (mGy/R or rad/R) conversion factor, L is the length of the pencil ion chamber (i.e., 100 mm), and T is the slice thickness (mm). It can be shown that this method is mathematically equivalent to using a small exposure meter and acquiring all 14 CT scans. The 100-mm pencil ion chamber cannot be used to measure the CTDI_{FDA} for slice thicknesses other than 7 mm.



Lucite CT dosimetry phantom

FIGURE 13-36. A diagram of a Lucite phantom, commonly used to determine dose in computed tomography (CT), is shown. The Lucite cylinder has holes drilled out for the placement of the CT pencil chamber. Lucite rods are used to plug in all remaining holes. A CT scan is acquired at the center of the cylinder, and dose measurements are made.

Ref: Bushberg 32

Radiation Dose in CT – effect of pitch

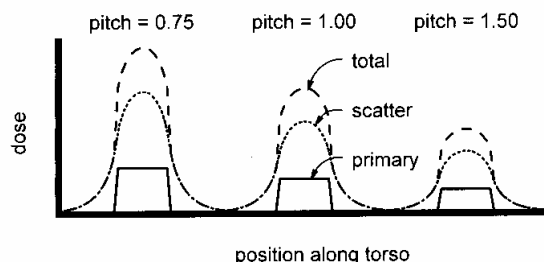


FIGURE 13-37. Dose profiles for three different collimator pitches are illustrated. A pitch of 1.0 corresponds to a dose profile very similar to that of an axial scan. For the same mAs and kV, a (collimator) pitch of 0.75 results in 33% more dose and a pitch of 1.5 corresponds to 66% less dose, compared with a pitch of 1.0. The primary, scatter, and total dose components are shown.

Ref: Bushberg 33

Radiation Dose in Helical CT

Dose Considerations in Helical Scanning

Helical scanning with a collimator pitch of 1.0 is physically similar to performing a conventional (nonhelical) axial scan with contiguous slices. For CT scanners with multiple detector arrays, the collimator pitch (not the detector pitch) should be used for dose calculations. The dose in helical CT is calculated in exactly the same manner as it is with axial CT, using the CTDI discussed in the previous section; however a correction factor is needed when the pitch is not 1.0:

$$\text{Dose (helical)} = \text{Dose (axial)} \times \frac{1}{\text{Collimator pitch}}$$

For example, with a collimator pitch of 1.5, the dose from helical scanning is 67% that of the dose from conventional scanning, and a collimator pitch of 0.75 corresponds to a helical dose that is 133% of the axial dose (i.e., 33% greater), assuming the same mAs was used (Fig. 13-37). It is important to keep in mind, as mentioned earlier, that the dose changes linearly with the mAs of the study.

Ref: Bushberg 34

Dose versus SNR, pixel size & slice thickness

In CT there is a well-established relationship among SNR, pixel dimensions (Δ) slice thickness (T), and radiation dose (D):

$$D \propto \frac{SNR^2}{\Delta^3 T}$$

The clinical utility of any modality lies in its spatial and contrast resolution.

Ref: Bushberg 35

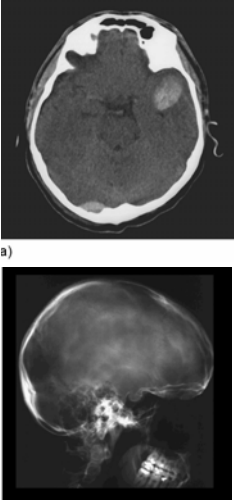
Contrast Resolution vs Spatial Resolution

Compared with x-ray radiography, CT has significantly worse spatial resolution and significantly better contrast resolution. The MTF, the fundamental measurement of spatial resolution, was shown in Fig. 13-30 for a typical CT scanner; it should be compared with the typical MTF for radiography, discussed in Chapter 10. Whereas the limiting spatial frequency for screen-film radiography is about 7 line pairs (lp) per millimeter and for digital radiography it is 5 lp/mm, the limiting spatial frequency for CT is approximately 1 lp/mm.

It is the contrast resolution of CT that distinguishes the modality: CT has, by far, the best contrast resolution of any clinical x-ray modality. Contrast resolution refers to the ability of an imaging procedure to reliably depict very subtle differences in contrast. It is generally accepted that the contrast resolution of screen-film radiography is approximately 5%, whereas CT demonstrates contrast resolution of about 0.5%. A classic clinical example in which the contrast resolution capability of CT excels is distinguishing subtle soft tissue tumors: The difference in CT number between the tumor and the surrounding tissue may be small (e.g., 20 CT numbers), but because the noise in the CT numbers is smaller (e.g., 3 CT numbers), the tumor is visible on the display to the trained human

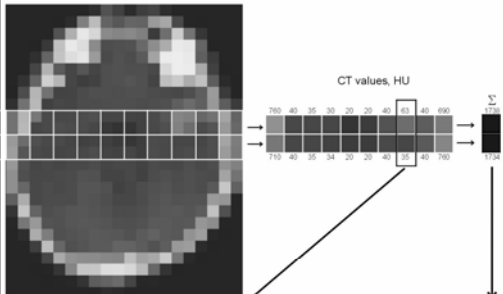
Ref: Bushberg 36

Computed Tomography – improved contrast over projection x-ray imaging with loss of spatial resolution



a)

b)



CT values, HU

CT image:

High local contrast of soft tissue structures

$$\text{contrast} = \Delta CT = I_1 - I_2 = 63 - 35 = 28\text{HU} \approx 50\%$$

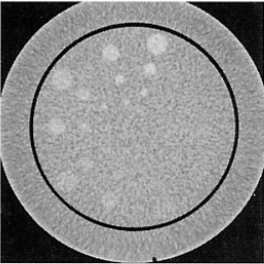
X-ray image:

Low contrast of soft tissue structures due to superposition of bones

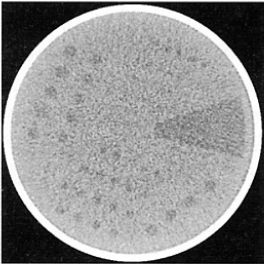
$$\text{contrast} = \frac{I_1 - I_2}{(I_1 + I_2) / 2} = \frac{1738 - 1734}{(1738 + 1734) / 2} \cdot 100\% = 0,23\%$$

Ref: Bushberg 37

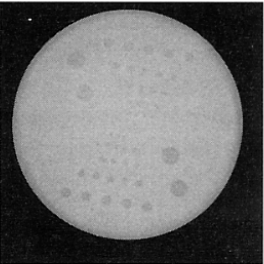
Contrast - Resolution analysis



a)



b)



c)

Figure 4.8
 Various phantoms are available for the measurement of low-contrast resolution, such as the Catphan (a), the ATS phantom (b) and the QRM LowC phantom (c). However, these may give contradictory results [Süß, 1999].

Ref: Kalender 38

Contrast - Resolution analysis

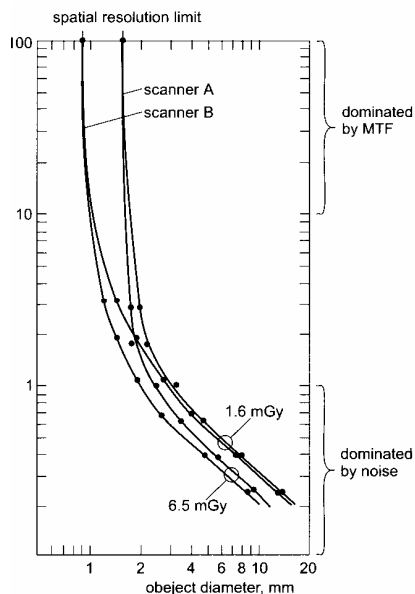


Figure 4.9

Contrast-detail diagrams reflect the influence of quantum noise and spatial resolution on the detectability of object details. For structures with contrast and diameter above or to the right of the respective curve, adequate resolution can be expected [Cohen, 1979].

Ref: Kalender 39

Factors Affecting Spatial Resolution

Detector pitch: The detector pitch is the center-to-center spacing of the detectors along the array. For third-generation scanners, the detector pitch determines the ray spacing; for fourth-generation scanners, the detector pitch influences the view sampling.

Detector aperture: The detector aperture is the width of the active element of one detector. The use of smaller detectors increases the cutoff (Nyquist) frequency of the image, and it improves spatial resolution at all frequencies.

Number of views: The number of views influences the ability of the CT image to convey the higher spatial frequencies in the image without artifacts (see Fig. 13-23). Use of too few views results in view aliasing, which is most noticeable toward the periphery of the image.

Number of rays: The number of rays used to produce a CT image over the same FOV has a strong influence on spatial resolution (see Fig. 13-22). For a fixed FOV, the number of rays increases as the detector pitch decreases.

Focal spot size: As in any x-ray imaging procedure, larger focal spots cause more geometric unsharpness in the detected image and reduce spatial resolution. The influence of focal spot size is very much related to the magnification of an object to be resolved.

Object magnification: Increased magnification amplifies the blurring of the focal spot. Because of the need to scan completely around the patient in a fixed-diameter gantry, the magnification factors experienced in CT are higher than in radiography. Magnification factors of 2.0 are common, and they can reach 2.7 for the entrant surfaces of large patients.

Slice thickness: The slice thickness is equivalent to the detector aperture in the cranial-caudal axis. Large slice thicknesses clearly reduce spatial resolution in the cranial-caudal axis, but they also reduce sharpness of the edges of structures in the transaxial image. If a linear, high-contrast object such as a contrast-filled vessel runs perfectly perpendicular to the transaxial plane, it will exhibit sharp edges regardless of slice thickness. However, if it traverses through the patient at an angle, its edges will be increasingly blurred with increased slice thickness.

Slice sensitivity profile: The slice sensitivity profile is quite literally the line spread function in the cranial-caudal axis of the patient. The slice sensitivity profile is a more accurate descriptor of the slice thickness.

Ref: Bushberg 40

Factors Affecting Spatial Resolution II

Helical pitch: The pitch used in helical CT scanning affects spatial resolution, with greater pitches reducing resolution. A larger pitch increases the width of the slice sensitivity profile.

Reconstruction kernel: The shape of the reconstruction kernel has a direct bearing on spatial resolution. Bone filters have the best spatial resolution, and soft tissue filters have lower spatial resolution.

Pixel matrix: The number of pixels used to reconstruct the CT image has a direct influence (for a fixed FOV) on spatial resolution; however no CT manufacturer compromises on this parameter in a way that reduces resolution. In some instances the pixel matrix may be reduced. For example, some vendors reconstruct to a 256×256 pixel matrix for CT fluoroscopy to achieve real-time performance. Also, in soft copy viewing, if the number of CT images displayed on a monitor exceeds the pixel resolution of the display hardware, the software downscans the CT images, reducing the spatial resolution. For example, a $1,024 \times 1,024$ pixel workstation can display only four 512×512 CT images at full resolution.

Patient motion: If there is involuntary motion (e.g., heart) or motion resulting from patient noncompliance (e.g., respiratory), the CT image will experience blurring proportional to the distance of the motion during the scan.

Field of view: The FOV influences the physical dimensions of each pixel. A 10-cm FOV in a 512×512 matrix results in pixel dimensions of approximately 0.2 mm, and a 35-cm FOV produces pixel widths of about 0.7 mm.

Ref: Bushberg 41

Factors Affecting Contrast Resolution

mAs: The mAs directly influence the number of x-ray photons used to produce the CT image, thereby affecting the SNR and the contrast resolution. Doubling of the mAs of the study increases the SNR by $\sqrt{2}$ or 41%, and the contrast resolution consequently improves.

Dose: The dose increases linearly with mAs per scan, and the comments for mAs apply here.

Pixel size (FOV): If patient size and all other scan parameters are fixed, as FOV increases, pixel dimensions increase, and the number of x-rays passing through each pixel increases.

Slice thickness: The slice thickness has a strong (linear) influence on the number of photons used to produce the image. Thicker slices use more photons and have better SNR. For example, doubling of the slice thickness doubles the number of photons used (at the same kV and mAs), and increases the SNR by $\sqrt{2}$, or 41%.

Reconstruction filter: Bone filters produce lower contrast resolution, and soft tissue filters improve contrast resolution.

Patient size: For the same x-ray technique, larger patients attenuate more x-rays, resulting in detection of fewer x-rays. This reduces the SNR and therefore the contrast resolution.

Gantry rotation speed: Most CT systems have an upper limit on mA, and for a fixed pitch and a fixed mA, faster gantry rotations (e.g., 1 second compared with 0.5 second) result in reduced mAs used to produce each CT image, reducing contrast resolution.

Ref: Bushberg 42

Artifacts – beam hardening

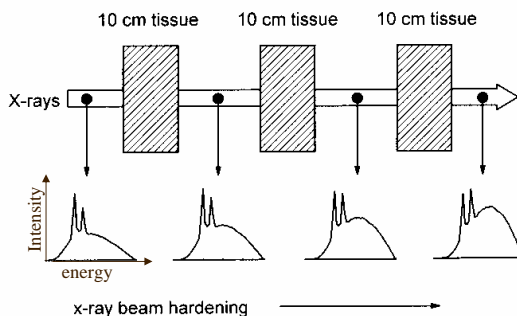


FIGURE 13-38. The nature of x-ray beam hardening is illustrated. As a spectrum of x-rays (**lower graphs**) passes layers of tissue, the lower-energy photons in the x-ray spectrum are attenuated to a greater degree than the higher-energy components of the spectrum. Therefore, as the spectrum passes through increasing thickness of tissue, it becomes progressively skewed toward the higher-energy x-rays in that spectrum. In the vernacular of x-ray physics, a higher-energy spectrum is called a "harder" spectrum; hence the term *beam hardening*.

Ref: Bushberg 43

Artifacts – beam hardening

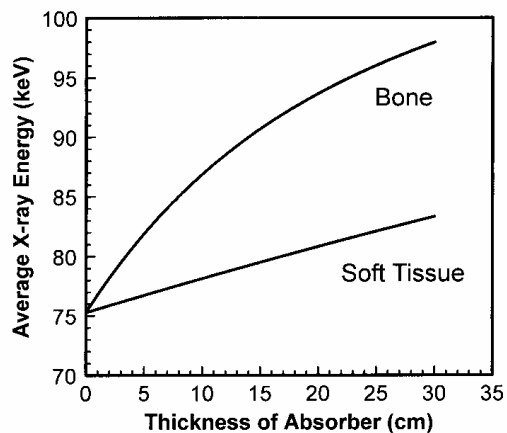


FIGURE 13-39. Using a 120-kV x-ray spectrum filtered by 7 mm of aluminum as the incident x-ray spectrum, the average x-ray energy of the spectrum is shown as a function of the thickness of the absorber through which the spectrum propagates. Beam hardening caused by soft tissue and by bone is illustrated. Bone causes greater beam hardening because of its higher attenuation coefficient (due to increased density and higher average atomic number).

Ref: Bushberg 44

Artifacts – beam hardening

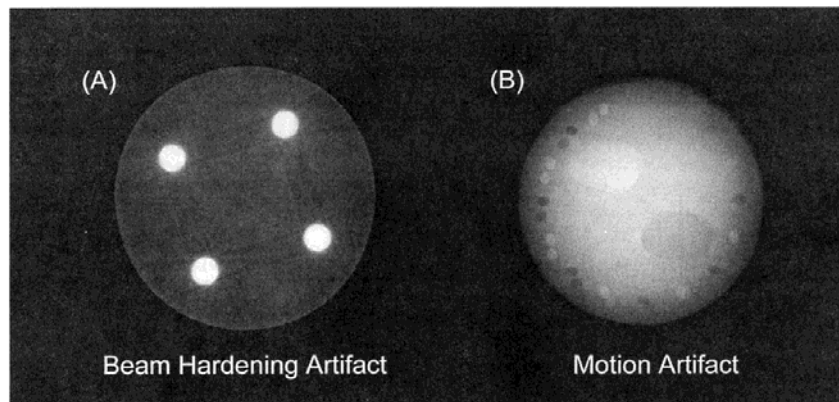


FIGURE 13-40. A: A beam-hardening artifact caused by four calcium-filled cylinders is illustrated. B: Artifacts due to motion are shown.

Ref: Bushberg 45

Artifacts – partial volume effects

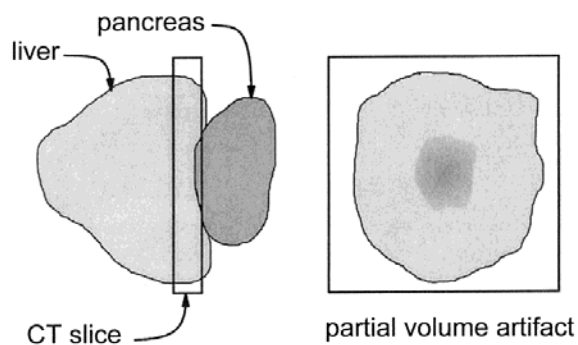


FIGURE 13-41. A partial volume artifact occurs when the computed tomographic slice interrogates a slab of tissue containing two or more different tissue types. Many partial volume artifacts are obvious (e.g., with bone), but occasionally a partial volume artifact can mimic pathologic conditions.

Ref: Bushberg 46

Artifacts –

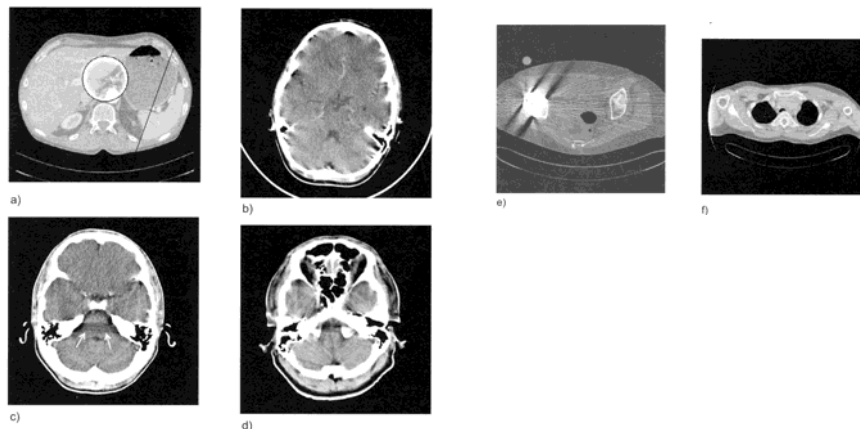


Figure 4.10
Typical examples for artifacts in CT images which may result from failures of the detector electronics (a), patient motion (b), beam hardening (c), partial volume effects (d), metallic implants (e) or the patient exceeding the field of measurement (f).

Ref: Bushberg 47

Projects – schedule...

Talk to me to define project BEFORE Oct 28

Report on outline of your project BEFORE Nov 12

- Including – outline of literature search
(words used in search, papers found, etc)
- endnote print out of all papers in search
(you read all abstracts of those listed)
 - list of papers skimmed in more detail.
 - list of papers read completely

Plan – papers to read in next two weeks
- work with B. Pogue on strategic changes.

Final report written by Dec 8 or before.

48